Journal of Stress Analysis
Vol. 9, No. 1, 2025, 27-35
Bu-Ali Sina University

ORIGINAL RESEARCH PAPER

Finite Element Simulations of the Effective Train in Monotonic and Cyclic High Pressure Torsion Procedures

Shokrolah Naseri[a], **Ali Mohammad Rashidi**[b,*], **Mohammad Hossein Yas**[a]

[a] Department of Mechanical Engineering, Razi University, Kermanshah, Iran.
[b] Department of Materials and Textile Engineering, Razi University, Kermanshah, Iran.

Article info

Article history:
Received 05 August 2024
Received in revised form
25 June 2025
Accepted 27 June 2025

Keywords:
Effective strain
HPT
Moment
Response surface method
Twisting angle amplitude

Abstract

No study has comparatively examined the impact of compressive loads in monotonic and cyclic high-pressure torsion (mHPT and cHPT) using the finite element analysis (FEA). This study aimed to overcome this lack of knowledge. For this purpose, the effect of compressive load on the saturated torque and effective strain imposed by mHPT and cHPT processes was investigated by finite element analysis of copper samples, under pressures of 100MPa and 150MPa and at three twist angles. The results demonstrated that in the mHPT process due to the increase in the compressive load the values of the effective strain and the maximum torque increased from 5.58 and 983N.m to 6.85 and 1967N.m, respectively. In contrast, the value of the effective strain imposed by cHPT ranged from 27.3 to 100.4 as the applied pressure-twist angle amplitudes increased from 100 MPa-1 rad to 150MPa-3 rad, respectively. Regardless of the applied load in mHPT, as the twist angle increased from about 1 rad to nearly 15 rad, the moment increased with a constant slope. In the cHPT procedure, the torque value was nearly independent of the number of cyclic revolutions, but it increased as the applied pressure and twist angle amplitudes increased. A 50% increase in applied load led to ∼23% and ∼88% increases in effective strain imposed by the mHPT and cHPT processes.

Nomenclature

E	Young's modulus	ρ	Density
h	Initial height	ν	Poisson's ratio
N	Number of revolutions	γ	Shear strain
N_c	Number of cycles	$\overline{\varepsilon}$	Effective strain
r	Initial radius	$\overline{\varepsilon}_{tor}$	Effective strains in shear deformation
t	Rotation time	$\overline{\varepsilon}_{up}$	Effective strains in upsetting
σ_y	Yield strength	$\overline{\varepsilon}_{cyc}$	Accumulated strain in cyclic deformation
ω	Twisting rate (angular velocity)	η	Efficiency factor
ϕ	Twisting angle	ε_f, ε_r	Forward and reverse imposed strains
ϕ_a	Twist angle amplitude	ε_1, ε_2, ε_3	principal strains

*Corresponding author: A. M. Rashidi (Associate Professor)
E-mail address: rashidi673@yahoo.com
10.22084/jrstan.2025.29720.1261
ISSN: 2588-2597

1. Introduction

Severe plastic deformation (SPD) processes, such as high-pressure torsion (HPT), are techniques in which material grain sizes are reduced to nanoscale dimensions and a high density of crystalline defects, such as dislocations, are created. As a result, the mechanical properties and microstructure of the materials are significantly improved [1,2]. Among the many SPD methods, HPT is widely used for studying the effects of creating severe strain in decreasing material grain sizes to the nanoscale on an academic scale, despite its limitations in industrial applications [3,4]. The design and manufacture of new materials and quasi-stable phases with advanced properties are also possible by combining this method with theoretical studies and computer simulations [5].

Numerous attempts have been made to improve the capabilities of HPT method [6-8]. One of these efforts has led to the development a reversed (cyclic) HPT process that has garnered significant attention in the last decade [9]. In conventional high-pressure torsion, the sample is twisted in only one direction. However, in the reversed HPT procedure, the sample was twisted to some extent in one direction and then twisted in the reverse direction. This process was carried out until a suitable cumulative strain was achieved in the sample. The conventional and reversed HPT procedures were monotonic and cyclic high-pressure torsion (mHPT and cHPT), respectively [10]. Research results on the Al-3%Mg-0.2Sc alloy indicated that applying cHPT decreased the sample edge hardness compared to mHPT [5]. Studies on Armco iron and Ni revealed that the applied moment reached a saturation limit value in both procedures as cumulative strain increased [9]. In cHPT, increasing the shear strain in a single cycle increases the saturated moment, which approaches the value obtained in mHPT. When the cumulative strain surpasses the saturation limit of mHPT, it forms finer grains than those obtained through cHPT. Similar findings have been reported in studies on pure aluminum [11], Al-Cu-Mg-Li alloy [12], and Fe-0.03C alloy [13]. In contrast to the aforementioned results, it has been reported that applying cHPT to pure aluminum [14], eutectoid Zn-22% Al alloy [15], and Ti-6Al-4V alloy [16] resulted in higher hardness and finer microstructure compared to the mHPT process. This inconsistency highlights the need for further research to comprehend the effects of the severe deformation process in cHPT.

Axial compressive load is an important technical parameter in the conventional high-pressure torsion process (mHPT). As the compressive load increases, the flow stress and dislocation density increase, resulting in finer grains [17]. The most significant effect of the compressive load is its impact on the strain corresponding to the maximum shear stress, which increases rapidly as the pressure increases. Applying a compressive load allows the sample to be twisted to a greater extent without breaking. In addition, increasing the compressive load at the same rotation speed increases the moment and shear stress that the sample can withstand without fracture [18].

The literature review indicates that the primary focus of research has on the cHPT procedure under a constant compression load, and there has been a lack of investigation on the effect of axial load on the effectiveness of the cHPT method. This study aims to fill this gap using FEA. It is well known that three-dimensional FEA is an effective alternative tool for evaluating the effective strain and insertion torque in metal deformation processes. It can provide a map of the strain distribution that is very difficult to obtain through laboratory tests [19]. In this regard, the effect of axial load on cumulative effective strain and torque in both mHPT and cHPT processes was investigated by FEA, and the results were compared. The main innovation of this study is that the obtained results reveal a stronger dependence of the cumulative effective strain and torque on the applied load in the cHPT process in comparison to the mHPT method, such that the percentage increase in cumulative effective strain due to a 50% increase in applied load in the cHPT process was ∼4.5 times greater than that in the mHPT method.

2. Theoretical Background of Equivalent Strain

Equivalent (effective) plastic strain is one of the most significant parameters typically investigated in SPD processes. It is a useful scalar quantity for comparing the effects of various severe plastic deformation methods. This scalar quantity equates to the effect of multiaxial strains created when applying a multiaxial stress state to the absolute value of the axial plastic strain in uniaxial tension or compression.

Generally, in the HPT process, a disk-shaped sample is placed inside the cylindrical cavities of the anvils, with the upper anvil pressed down on it, after which the lower anvil is rotated relative to the upper anvil under high pressure. Consequently, intense shear strain is imposed through the simple shear deformation mode. Assuming that the sample's thickness does not change during the shearing deformation, the imposed engineering shear strain γ can be expressed in the form of the following relationship [20] :

$$\gamma = \frac{r\phi}{h} \tag{1}$$

Here, ϕ represents the twisting angle (Rad), and h and r refer to the disk's initial height and initial radius, respectively. The twisting angle (in radians) can be expressed as:

$$\phi = 2N\pi = \omega t \tag{2}$$

Therefore, Eq. (2) can be rewritten as follows

$$\gamma = \frac{r\phi}{h} = 2N\pi\frac{r}{h} = \frac{r}{h}\,\omega t \tag{3}$$

Here, N represents the number of revolutions, ω is the twisting rate (angular velocity in radians per second), and t indicates the rotation time (in seconds).

The calculation of the effective strain corresponding to shear strain γ depends on the criteria used for the effective stress. Over the past few years, researchers have focused on two main approaches as appropriate criteria for interpreting effective strain: von Mises equivalent strains and Hencky logarithmic strains.

Generally, when a sample is deformed under the multiaxial state of stress with a constant ratio of $d\varepsilon_1$:$d\varepsilon_2$:$d\varepsilon_3$, the effective strain ($\bar{\varepsilon}$) for the von Mises criterion can be expressed as follows [21]:

$$\bar{\varepsilon}=\sqrt{\frac{2}{3}({\varepsilon_1}^2+{\varepsilon_2}^2+{\varepsilon_3}^2)} \tag{4}$$

However, since $\varepsilon_2 = 0$; $\varepsilon_1 = -\varepsilon_3 = \frac{1}{2}\gamma$ in torsional deformation, based on the von Mises criterion, effective strains corresponding to the shear strain imposed during HPT, $\bar{\varepsilon}_{tor}$, can be estimated using Eq. (5):

$$\bar{\varepsilon}_{tor}=\frac{\gamma}{\sqrt{3}}=\frac{r\phi}{\sqrt{3}h} \tag{5}$$

Hencky [22] proposed that using the logarithmic form is preferable for expressing the effective strains in large deformations. Therefore, regarding the Hencky criterion, $\bar{\varepsilon}_{tor}$ can be analyzed using Eq. (6):

$$\bar{e}_{tor}= \ln\gamma \tag{6}$$

Later, several researchers such as Tekkaya [23] and Onaka [24] have demonstrated that the modified version of the Hencky equation (Eq. (7)) is more preferable for calculating the equivalent strain for large shear strains where $\gamma > 0.8$.

$$\bar{\varepsilon}_{tor} = \frac{2}{\sqrt{3}}\ln\left(\sqrt{1+\frac{\gamma^2}{4}}+\frac{\gamma}{2}\right) \tag{7}$$

In practice, $\gamma \gg 1$ for HPT, and as a result, the modified Hencky equation can be simplified in the following form:

$$\bar{e}_{tor} = \frac{2}{\sqrt{3}}\ln(\gamma) \;= \frac{2}{\sqrt{3}}\ln\left(\frac{r_o\phi}{h_o}\right) \;= \frac{2}{\sqrt{3}}\ln(\omega t\frac{r_o}{h_o}) \tag{8}$$

Under deformation by the ideal constrained HPT method, the material flow in the axial and radial directions is restricted by anvils, and the dimensions of the sample remain constant during processing. This means that $\varepsilon_2 = 0$; $\varepsilon_1 = -\varepsilon_3 = \frac{1}{2}\gamma$ and the sample is only subjected to simple shear deformation. Therefore, the previously presented equations can be used for an ideally constrained HPT process. In contrast, when the sample is subjected to unconstrained HPT, the material flows in the direction of the thickness and radius of the sample.

To estimate the accumulated effective strain, it is necessary to incorporate the compressive strain resulting from axial loading. Therefore, the total effective strain can be expressed as [25].

$$\bar{\varepsilon} = \bar{\varepsilon}_{tor} + \bar{\varepsilon}_{up} \tag{9}$$

Where $\bar{\varepsilon}_{tor}$ and $\bar{\varepsilon}_{up}$ are effective strains corresponding to the imposed simple shear strain and the compressive strain introduced during the upsetting of the sample, respectively. The latter can be calculated by the equation$\bar{\varepsilon}_{up}= \ln\frac{h_o}{h}$ and the former can be obtained from each equation presented earlier.

The equations mentioned above has been proposed to estimate the accumulated effective strain in the mHPT processes. Stuwe [26] has defined an efficiency factor, $0< \eta< 1$, for the cyclic deformation process as follows:

$$\eta = \frac{\sum_1^{N_c}\varepsilon_i}{\bar{\varepsilon}_{cyc}} = \frac{\sum_1^{N_c}(|\varepsilon_f|+|\varepsilon_r|)}{\bar{\varepsilon}_{cyc}} \tag{10}$$

Where $\bar{e}_{cyc}$ represents the accumulated strain in cyclic deformation, N_c is the number of cycles, e_i is the total strain induced during cycle i, and e_f and e_r are the true strains imposed in the forward and reverse directions during each cycle of the deformation process. Regarding the von Mises or Hencky criterion, the values e_f and e_r can be analyzed isong Eq. (5) or Eq. (9), respectively. As a result, the accumulated effective strain in the cyclic unconstrained HPT processes can be estimated as follows:

$$\bar{\varepsilon}_{cyc} = \ln\frac{h_o}{h} + \frac{\eta}{\sqrt{3}}\frac{r_o\phi}{h_o} \qquad \text{for von Mises criterion} \tag{11}$$

$$\bar{\varepsilon}_{cyc} = \ln\frac{h_o}{h} + \frac{2\eta}{\sqrt{3}}\ln\left(\frac{r_o\phi}{h_o}\right) \qquad \text{for Hencky criterion} \tag{12}$$

Here, ϕ is the twisting angle equated to the twisting angles in the forward (ϕ_f) and reversed (ϕ_r) directions in each cyclic deformation, and it can be calculated using Eq. (13).

$$\phi = \sum_1^N(|\phi_f|+|\phi_r|) \tag{13}$$

3. Materials and Methods

3.1. Materials

Pure copper was used in this research as a work metal because its deformation behavior during the

HPT process has been thoroughly studied by Jahedi et al. [27]. The material properties were taken as follows: ρ= 8.9×10^{3}kg/m^3, E= 120GPa, ν= 0.36, and s_y= 70MPa. Also, the proposed true stress-true strain relationship, i.e., σ (MPa) = 330$\varepsilon^{0.235}$, was employed in this study. A rod with a length of 25mm and an initial diameter of 24mm was used as the workpiece. To avoid stress concentration on both sides of the rod, surface turning and chamfering were applied to the middle 18mm section.

3.2. Finite Element Analysis

Three-dimensional (3D) finite element analysis of the monotonic and cyclic HPT processes was conducted using Abaqus/Explicit, a general method for modeling large deformations of materials. To verify the simulation method employed in this study, and to ensure that valid results are obtained by this method, in the first step, the modeling process was adjusted and evaluated by simulating HPT using a cylindrical sample of pure copper with identical geometry and properties as those mentioned in Ref [27]. All conditions were the same except for the proposed mesh size, contributing to slower program execution and longer running time. Therefore, several mesh sizes were tested. Finally, a value was chosen as the appropriate mesh size, resulting in responses comparable to the experimental data [27] with the shortest running time. Table 1 compares the results obtained with those reported by Jahedi et al. [27]. As can be seen, the relative differences between the obtained and reported FEA results are approximately 6.2%, 1.8%, and 0.5% for the maximum equivalent plastic strain, final thickness, and final diameter, respectively, which demonstrate excellent agreement between the FEA results of both studies. Moreover, the simulation method employed in this study showed good agreement with the reported experimental results [27].

Selecting an appropriate mesh size is a critical task in FEM. Literature reviews indicated that a typical approach is the initial FE analysis of a basic variable in the problem for several different mesh sizes. Typically, as the mesh number increases the solution tends towards a unique value, so the change in results is not significant with further mesh refinement. Herein, FE analysis was performed on specimens meshed with different numbers of C3D8R elements ranging from 336 to 23712. The torque-twist curves of the samples subjected to the mHPT process under an applied load corresponding to the initial pressure of 100MPa were taken into consideration. The resultant diagrams are compared in Fig. 1. As seen, the torque-twist curves for samples meshed with 1008, 3384, and 6864 elements are in close proximity to one another.

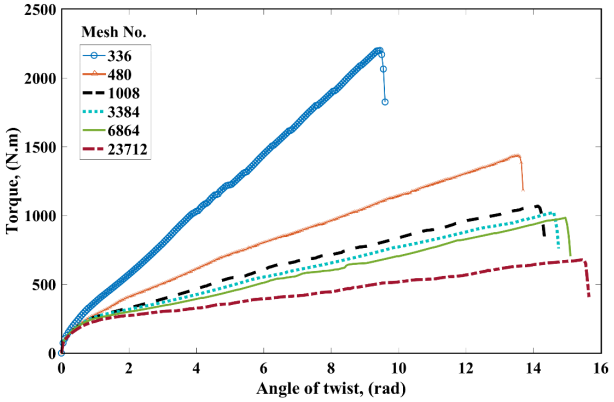

Fig. 1. Mesh number influence on the torque-twist curve for mHPT performed under initial pressure of 100MPa.

Regarding the results presented in Fig. 1, mHPT and cHPT were initially simulated using 3008 C3D8R elements to save computation time and cost, but it resulted in the severe distortion of the simulated specimens, which appeared at large twists. Therefore, in the final step, the mHPT and cHPT processes were modelled using the samples meshed with 6864 C3D8R elements. The unmeshed and initially meshed workpieces are presented in Fig. 2. One side of the rod was fully fixed. The midpoint of the surface of the other side was selected as a reference point. It is subjected to a reversible torsional force and gradually twisted around the long axis with an angular velocity of 1rad/s. According to the preliminary simulation results illustrated in Fig. 1, the torque required to twist the object first increased gradually and then suddenly dropped. The simulated images of the deformed samples also showed that further torsion led to noticeable deformation fluctuations and breakdown at the connection between the flat part of the sample and its head. This phenomenon may have been caused by an increase in stress concentration at the connection point and by its value reaching the material's fracture strength. For this reason, the analysis process was continued until the sudden drop in torque, which was taken as a failure criterion.

Table 1
Comparison of the obtained results with those reported [27].

Equivalent strain		Final thickness of specimen (mm)			Final diameter of specimen (mm)		
FEA Present study	FEA Reported	FEA Present study	FEA Reported	Experiment Reported	FEA Present study	FEA Reported	Experiment Reported
30	32	3.25	3.19	2.90±0.15	22.74	22.85	23.00±0.15

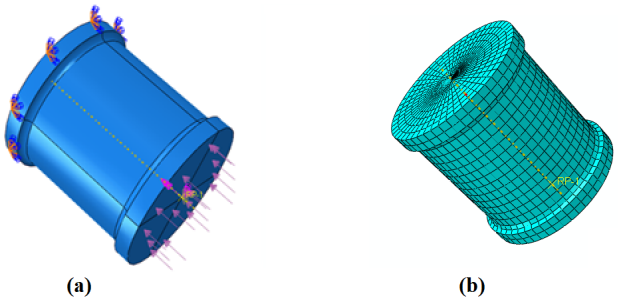

Fig. 2. Schematic view of the a) Unmeshed sample, and b) Initially meshed sample.

The output data were the effective strain and torque required to twist the sample. The key input data were the material properties, geometric dimensions of the sample, strain-hardening function, and compressive forces of 38000N and 57000N, equivalent to initial pressures of 100MPa and 150MPa, respectively, applied to the reference point of the revolved side. Another parameter that can significantly affect the behavior of a sample undergoing cHPT deformation is the twist angle amplitude, ϕ_a, during each deformation cycle. Here, it was assumed that the forward and reverse ϕ_a were equal. The $\phi_a$values of ±1, ±2, and ±3 radians were considered in the cHPT process modeling.

4. Results and Discussion

4.1. FEA Results of mHPT

Figs. 3a and 3b demonstrate the FE simulation results of samples twisted using the mHPT process up to the maximum allowable twist angles without failure under compressive loads corresponding to initial pressures of 100 and 150MPa, respectively.

As shown in Fig. 3a, the effective strain is minimum at the center of the sample, as expected, while it reaches its maximum value at the ends. The effective strains of 5.58 and 6.85 were obtained without failure under applied pressures of 100 and 150MPa, respectively. According to these values, a 50% increase in the applied compressive load resulted in an approximately 23% increase in the maximum effective strain imposed by the mHPT process. The effective strain values derived via FEA are the sum of effective strains associated with shear and compressive deformation (Eq. (11)). These values are much higher than those estimated using Eq. (10) (Hencky criterion), but are close to the values predicted by Eq. (7) (Mises criterion).

The changes in the moment with respect to the twisting angle for the samples subjected to pressures of 100 and 150MPa are depicted in Fig. 3. It is evident that up to approximately 14rad, there was a slight difference between the results obtained for the applied loads. Regardless of the applied loads, the moment value initially increased with a descending slope as the rotation angle increased, and then its slope remained almost constant up to nearly 15rad. Subsequently, the torque of the sample under 100MPa dropped sharply, while for the sample under 150MPa, it increased with an ascending slope until the sample failed. According to Fig. 4, a 50% increase in the applied compressive load resulted in an approximately 200% increase in the maximum torque in the mHPT process.

4.2. FEA Results of the cHPT

Fig. 5 shows the distribution patterns of accumulated strain corresponding to the maximum rotation number without failure of samples subjected to cHPT with a twisting rate of 1rad/s and a twist angle amplitude (ϕ_a) of 1rad, under initially applied pressures of 100 and 150MPa. It can be observed that the distribution of accumulated strain under both loads follows nearly the same trend in the cHPT procedure: a nearly symmetrical pattern with significantly high strain at the lower and upper ends of the samples. The accumulated strain values for applied pressures of 100MPa and 150MPa were approximately 27.3 and 41.2, respectively. This demonstrates that a 50% increase in the applied load led to a nearly 51 % increase in the accumulated strain when the sample was subjected to cHPT with a $\phi_a = 1\ rad$.

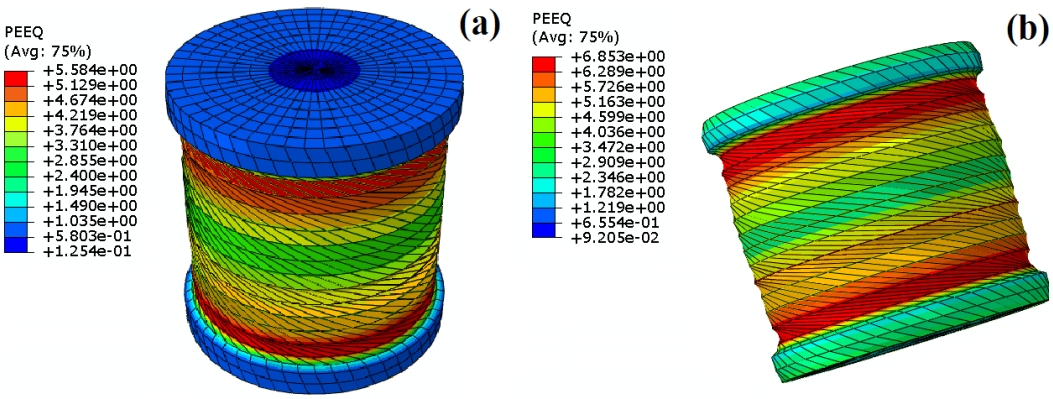

Fig. 3. Cumulative strain maps corresponding to the tolerable rotation number without failure of the sample subjected to the mHPT process with a $\omega = 1\frac{\text{rad}}{\text{s}}$ and an applied pressure of a) 100MPa, and b) 150MPa.

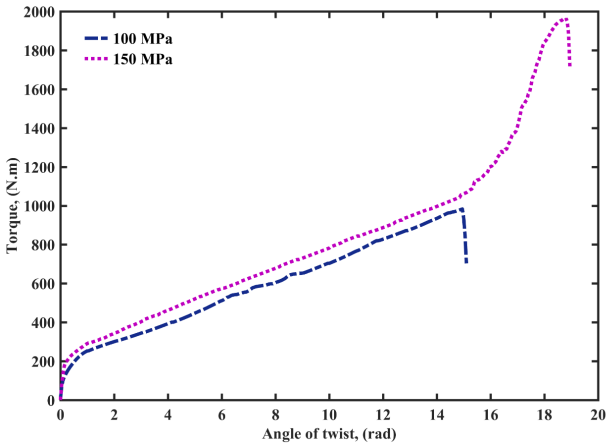

Fig. 4. Moment in terms of twist angle in mHPT procedure for $\omega = 1$rad/s, and applied pressures 100 and 150MPa.

This is 2.2 times higher than that obtained for the mHPT process. Furthermore, the maximum amounts of accumulated strain imposed on the cHPT samples were approximately 4.9 and 6 times greater than those of the mHPT samples under applied pressures of 100 and 150MPa, respectively.

The strain distribution patterns of samples under the cHPT procedure, with an initially applied pressure of 100MPa and twist angle amplitudes ϕ_a of 2 rad and 3rad, are illustrated in Fig. 6. It is evident that increasing the ϕ_a value results in more severe strains in multiple parts of the samples, and the maximum strain value also increases. This behavior was also observed in samples subjected to cHPT under a pressure of 150MPa.

Fig. 7 demonstrates the impact of the twist angle amplitude on the accumulated strain and the maximum cycle number before failure of the samples. The results indicate that increasing ϕ_a results in a decrease in the maximum cycle number, but it significantly increases the accumulated strain. Moreover, at high ϕ_a, the applied pressure had a more significant impact on the accumulated strain created during cHPT than at low ϕ_a. For example, the accumulated strain imposed by cHPT with $\phi_a = 3$ *rad* was approximately 54.2 and 100.4, for applied pressures of 100 MPa and 150MPa, respectively. A comparison of these values with those obtained for $\phi_a = 1$ *rad* shows a higher sensitivity to ϕ_a, as the compressive load increased; thus, a 50% rise in pressure led to a nearly 51% to approximately 86% change in the accumulated strain created by cHPT with ϕ_a of 1 rad to 3 rad, respectively.

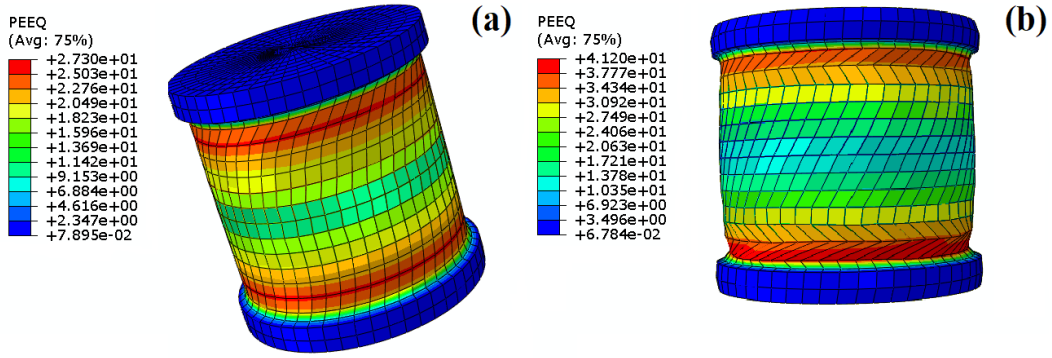

Fig. 5. Accumulated strain distribution in a sample subjected to cHPT deformation with = 1rad/s, and twist angle amplitude of 1 rad under pressure of a) 100MPa, 86 cycles, and b) 150MPa, 128 cycles

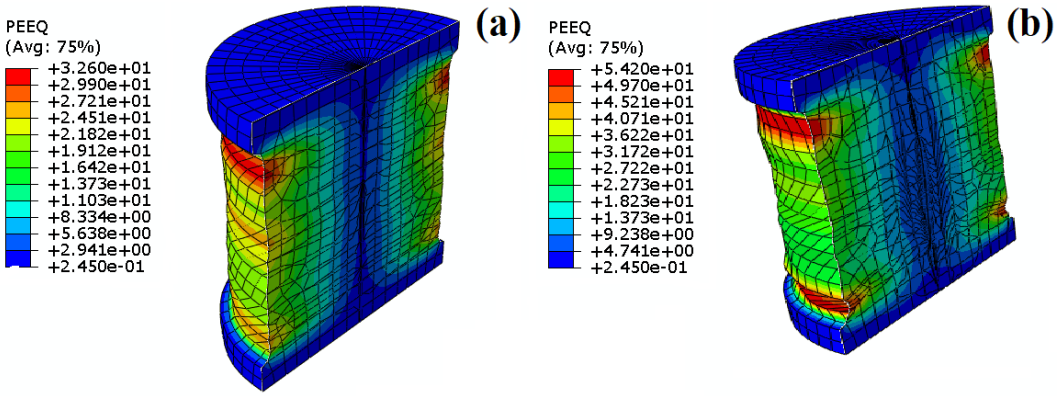

Fig. 6. Cumulative strain distribution in cHPT procedure under pressure of 100MPa and $\omega = 1$rad/s, with twist angle amplitude of a) 2rad, N=47 cycles, and b) 3rad, N=42 cycles.

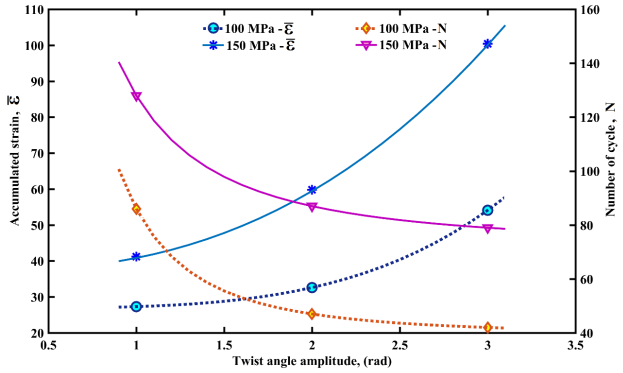

Fig. 7. Variation of accumulated strain with twist angle amplitude in cHPT procedure under the initial pressure of 100 and 150MPa (ω = 1rad/ss).

The average values of the height reduction, Δh, during the mHPT and cHPT processes were about 0.48mm and 2.1mm, respectively. By substituting these values, as well as the number of cycles corresponding to the maximum torque value into formulas 13 to 15, the values of efficiency factor, η, were calculated. The results showed that the Hencky criterion leads to high values of 5 to 15 which is unreasonable. Based on the von Mises criterion, an increase in pressure had no effect on η, but an increase in ϕ_a from 1 radian to 3 radians caused an increase in η from about 0.46 to nearly 0.61.

Typicallym, the first 20 s of the torque-twist curve for cHPT performed under different conditions with ω=1 rad/s are shown in Figs. 8a to 8d. For both pressures of 100 and 150MPa, the moment graphs exhibited regular periodicity in terms of time, and the desired maximum moment in each period was close to the maximum value of the previous and next periods. Similar behaviors were also observed in the samples twisted with $\phi_a = 2\ rad$ and ϕ_a = 3rad.

The plot in Fig. 9 shows the variations in the maximum torque values with respect tothe twist amplitudes. It is observed that the maximum applied torque increases with an increase in the compressive load and twisting domain. Specifically, as ϕ_a increased from 1 rad to 3rad, the maximum required moment increased from 426N.m to 518N.m and from 474N.m to 564N.m for the initially applied pressures of 100MPa and 150MPa, respectively. These values were significantly lower than those obtained from the FEA of the mHPT procedure (Fig. 4).

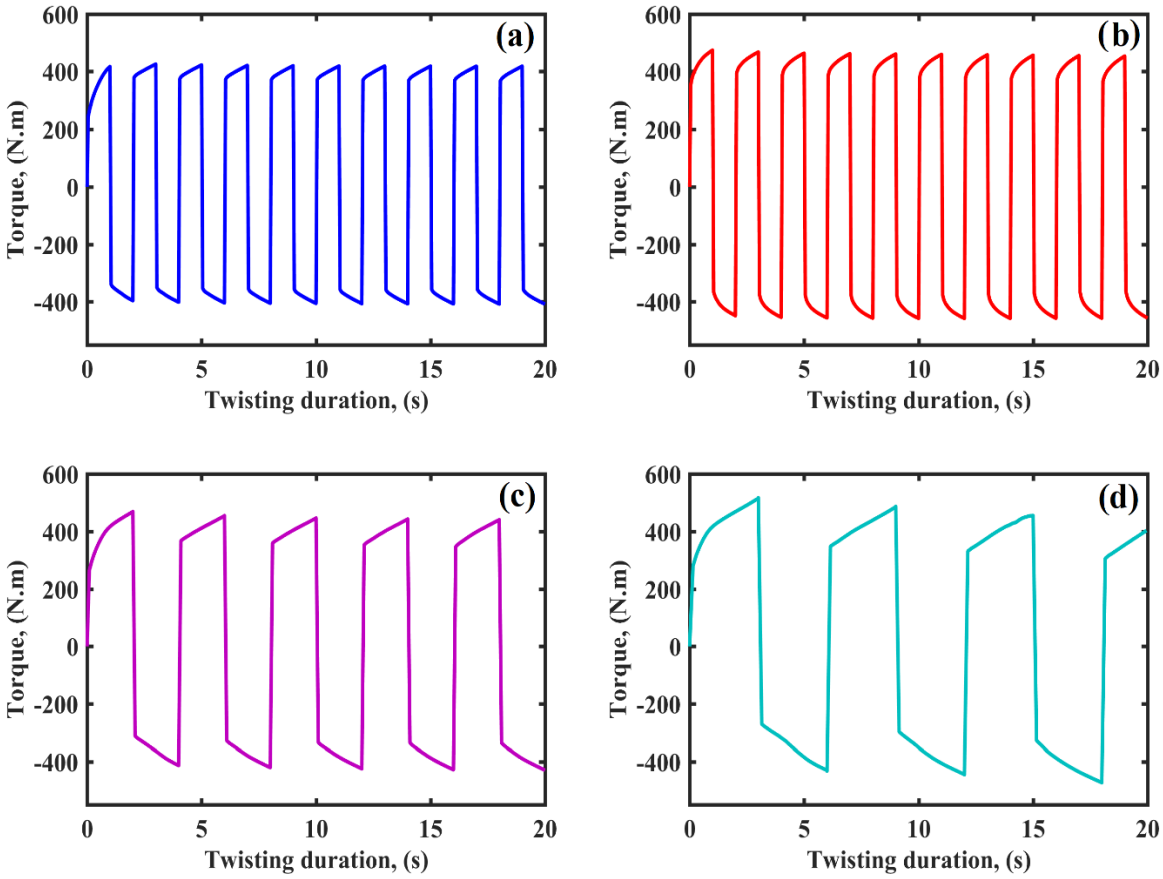

Fig. 8. Typical moment plots in cHPT procedure, a) P = 100MPa, ϕ_a = 1 rad, b) P = 150MPa, ϕ_a = 1rad, c) P = 100MPa, ϕ_a = 2rad, d) P = 100MPa, ϕ_a = 3rad.

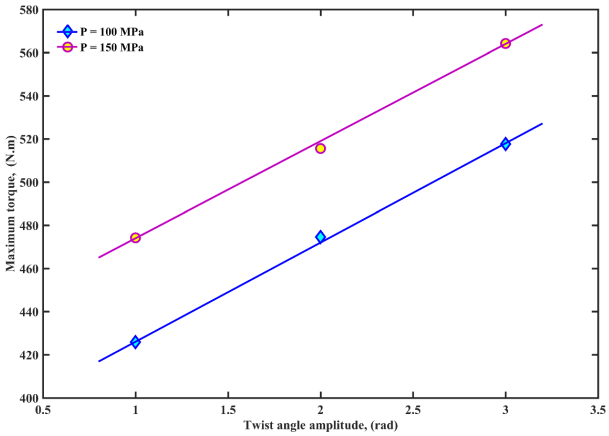

Fig. 9. Moment in terms of twist angle amplitudes in the cHPT procedure for $\omega = \pm 1$rad/s, and pressures of 100MPa and 150MPa.

5. Conclusion

The present study investigated the effect of compressive loading on monotonic and cyclic high-pressure torsion (HPT) processes using finite element simulations conducted by ABAQUS software. The key findings of this study are summarized as follows:

1. The effective strains created by mHPT deformation of copper under 100 MPa and 150 MPa pressures were 5.58 and 6.85, respectively.

2. In the mHPT process, there was no noticeable difference in the torque required to twist the sample to 15rad under loads of 100MPa and 150MPa. However, the maximum torque under a load of 150MPa was more than 2 times greater than that under a load of 100MPa.

3. By increasing the twist angle amplitude from 1rad to 3rad, the accumulated strain created by the cHPT procedure increased from 27.3 to 54.1 and from 41.2 to 100.4 for applied pressures of 100MPa and 150MPa, respectively.

4. The torque required for twisting the sample in cHPT is almost independent of the number of rotation cycles but it increases with an increase in the applied compressive load and twist angle amplitude from 426N.m to 564N.m, which are 2.3 and 1.7 times lower than the maximum moment in mHPT under 100MPa.

References

[1] R. Z. Valiev, B. Straumal, T. G. Langdon, Using Severe Plastic Deformation to Produce Nanostructured Materials with Superior Properties, Ann. Rev. Mater. Res., 52 (2022) 357-382.

[2] L. M. Reis, A. Hohenwarter, M. Kawasaki, R. B. Figueiredo, Evaluating high, Pressure torsion scale-up. Adv. Eng. Mater., (2024) 2400175.

[3] K. Edalati, A. Q. Ahmed, S. Akrami, K. Ameyama, V. Aptukov, R. N. Asfandiyarov, Y. T. Zhu, Severe plastic deformation for producing superfunctional ultrafine-grained and heterostructured materials: An interdisciplinary review, J. Alloys and Compounds, 1002 (2024).

[4] R. B. Figueiredo, M. Kawasaki, T. G. Langdon, The role of grain size in achieving excellent properties in structural materials, J. Mater. Res. Technol., 30 (2024) 3448-3462.

[5] Z. Horita, T.G. Langdon, Microstructures and microhardness of an aluminum alloy and pure copper after processing by high-pressure torsion, Mater. Sci. Eng., A410 (2005) 422-425.

[6] G. Kumar, P. Huilgol, S. Suwas, L. S. Toth, S. V. Kailas, Validation of the new high-pressure compressive reverse shearing severe plastic deformation process with the help of textures and microstructures, Mater. Charac., 224 (2025) 115013.

[7] C. T. Wang, Z. Li, J. T. Wang, T. G. Langdon, Recent developments in the use of high pressures for the production of nanostructured materials, Adv. Eng. Mater., 26 (2024) 2400477.

[8] C. T Wang, Z. Li, J. T. Wang, T. G. Langdon, Recent Developments in the Use of High Pressures for the Production of Nanostructured Materials, Adv. Eng. Mater., 26 (2024) 19.

[9] F. Wetscher, R. Pippan, Cyclic high-pressure torsion of nickel and Armco iron. Philos. Mag., 86 (2006) 5867-5883.

[10] F. Wetscher, R. Pippan, Hardening and softening behavior by cyclic high-pressure torsion, Metall. Mater. Trans. A, 40 (2009) 3258-3263.

[11] D. Orlov, Y. Todaka, M. Umemoto, N. Tsuji, Role of strain reversal in grain refinement by severe plastic deformation, Mater. Sci. Eng. A, 499(1-2) (2009) 427-433.

[12] J. W. Zhang, M. J. Starink, N. Gao, W. L. Zhou, Influence of strain reversals during high pressure torsion process on strengthening in Al-Cu-Mg (-Li) alloy, Mater. Sci. Forum, 667 (2010) 809-814.

[13] Y. Todaka, M. Umemoto, A. Yamazaki, J. Sasaki, K. Tsuchiya, Effect of strain path in high-pressure torsion process on hardening in commercial purity titanium, Mater. Trans., 49(1) (2008) 47-53.

[14] M. Kawasaki, B. Ahn, T. G. Langdon, Effect of strain reversals on the processing of high-purity aluminum by high-pressure torsion, J. Mater. Sci., 45 (2010) 4583-4593.

[15] M. Kawasaki, B. Ahn, T. G. Langdon, Significance of strain reversals in a two-phase alloy processed by high-pressure torsion, Mater. Sci. Eng. A, 527(26) (2010) 70087016.

[16] X. Ma, F. Li, J. Cao, J. Li, H. Chen, C. Zhao, Vickers microhardness and microstructure relationship of Ti-6Al-4V alloy under cyclic forward-reverse torsion and monotonic torsion loading, Mater. Design., 114 (2017) 271281.

[17] M. J. Zehetbauer, H. P. St́uwe, A. Vorhauer, E. Schafler, J. Kohout, The role of hydrostatic pressure in severe plastic deformation, Adv. Eng. Mater., 5(5) (2003) 330337.

[18] P. W. Bridgman, On torsion combined with compression, J. Appl. Phys., 14(6) (1943) 273283.

[19] P. Henrique, R. Pereira, R. B. Figueiredo, Finite Element Modelling of High-Pressure Torsion: An Overview, Mater. Trans., 60(7) (2019) 1139-1150.

[20] K. Edalati, Z. Horita, A review on high-pressure torsion (HPT) from 1935 to 1988, Mater. Sci. Eng., A652 (2016) 325-352.

[21] W. F. Hosford, R. M. Caddell, Metal Forming, Mechanics and Metallurgy, 4th Edition, Cambridge University Press, New York, (2011).

[22] H. Hencky, Uber die Form des Elastizitatsgesetzes bei ideal elastischen Stoffen, Zeit. Techn. Phys., 9 (1928) 215-220.

[23] A. E. Tekkaya, Equivalent strain and stress history in torsion tests, Steel Res., 65(2) (1994) 65-70.

[24] S. Onaka, Appropriateness of the Hencky equivalent strain as the quantity to represent the degree of severe plastic deformation, Mater. Trans., 53(8) (2012) 1547-1548.

[25] M. V. Degtyarev, T. I. Chashchukhina, L. M. Voronova, A. M. Patselov, V. P. Pilyugin, Influence of the relaxation processes on the structure formation in pure metals and alloys under high-pressure torsion, Acta Mater., 55(18) (2007) 6039-6050.

[26] H. P. St́uwe, Equivalent strain in severe plastic deformation, Adv. Eng. Mater., 5(5) (2003) 291-295.

[27] M. Jahedi, M. Knezevic, M. H. Paydar, High-pressure double torsion as a severe plastic deformation process: experimental procedure and finite element modeling, J. Mater. Engin. and Perform., 24 (2015) 1471-1482.